PROCEEDINGS OF SCIENCE

Charm and charmonia production in fixed-target collisions with LHCb

Juliette Authier[a,*]

[a] *Laboratoire Leprince-Ringuet, École polytechnique, Institut Polytechnique de Paris, CNRS/IN2P3, Palaiseau, France*

E-mail: juliette.authier@cern.ch

The production of charm quarks and charmonium states in fixed-target collisions provides a powerful probe of QCD in cold and hot nuclear matter. The LHCb experiment has pioneered a novel fixed-target program, now enhanced for Run 3 with the SMOG2 system, which features improved gas confinement and the capability to inject both noble and non-noble gases. This upgrade significantly increases fixed-target luminosity, enabling high-statistics studies of charm production in proton-nucleus (pA) and lead-nucleus (PbA) collisions. Charm production measurements in this environment offer unique insights into cold nuclear matter effects, such as nuclear PDF modifications, parton energy loss, and intrinsic charm contributions, across small and large collision systems at the same center-of-mass energy per nucleon pair ($\sqrt{s_{NN}}$). Additionally, these measurements provide an opportunity to investigate potential signatures of hot nuclear matter effects at lower energies. Results on open and hidden charm production using the pNe and PbNe datasets collected with SMOG are presented, as well as future prospects for charm studies in fixed-target collisions with SMOG2.

The European Physical Society Conference on High Energy Physics (EPS-HEP2025)
7-11 July 2025
Marseille, France

*Speaker

 ISSN 1824-8039 . Published by SISSA Medialab.

PoS(EPS-HEP2025)192

1. Introduction

Charm–anticharm quark pairs are produced at the earliest stage of the collision, and subsequently hadronize either into a charmonium state or into open-charm hadrons. Among the latter, the D^0 meson is the most abundantly produced and can therefore serve as a proxy for the overall charm quark production. The D^0 meson is also a powerful probe to study hadronization mechanisms and to explore the possible presence of intrinsic charm in the nucleon, due to its sensitivity to the initial partonic content. In addition, D^0 production provides an essential reference for the study of charmonium states, which are sensitive to both cold nuclear matter effects and to the hot and dense medium created in heavy-ion collisions. The combined study of open and hidden charm production therefore offers a comprehensive picture of charm quark dynamics, from their initial production to their interactions with the surrounding medium.

2. The LHCb experiment

The LHCb detector is a single-arm forward spectrometer. Its geometry covers the pseudorapidity region $2 < \eta < 5$. Its subdetectors provide a precise reconstruction of primary and secondary vertices, excellent tracking performances down to low p_T and high-quality particle identification [1, 2]. A distinctive feature of LHCb is its ability to operate both as a collider and as a fixed-target experiment. During the Run 2 of the LHC, fixed-target collisions were achieved thanks to the System for Measuring the Overlap with Gas (SMOG) [3] which allows the injection of noble gases into the beam pipe around the interaction point. In this configuration, the center-of-mass energy is significantly reduced, ranging from $\sqrt{s_{NN}} = 68.5$ to 113 GeV for beam energies between 2.5 and 6.8 TeV. Due to the boost of the beam, the rapidity in the center-of-mass of the reaction is shifted to $-2.5 \leq y^* \leq 0$, giving access to the high Bjorken-x region of the target ($10^{-2} \lesssim x_2 \lesssim 4 \times 10^{-1}$) at intermediate Q^2. This region of phase space, only partially explored by the other LHC experiments, offers ideal conditions for studying charm production.

3. Results on open charm production

The hadronization of quarks into hadrons is commonly described by fragmentation functions, whose parameters are determined from e^+e^- collision data and assumed to be universal accross collision systems. However, in nucleon–nucleon and nuclear collisions, valence quarks from the initial nucleons can participate in the hadronization process through a mechanism known as coalescence [4]. When a $c\bar{c}$ pair is produced at large rapidity, it may recombine with a valence quark, inducing an asymmetry between D^0 and $\overline{D}^0$ production. Such mechanism is particularly relevant in fixed-target collisions, where high Bjorken-x partons are involved.
The D^0-$\overline{D}^0$ production asymmetry has been measured in fixed-target pNe collisions by LHCb during the Run 2 of the LHC [5]. It is quantified as

$$\mathcal{A} = \frac{Y_{corr}(D^0) - Y_{corr}(\overline{D}^0)}{Y_{corr}(D^0) + Y_{corr}(\overline{D}^0)}, \tag{1}$$

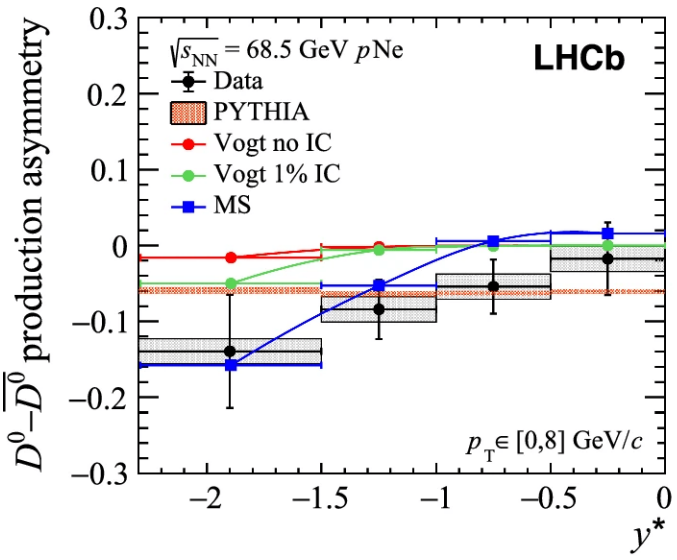

Figure 1: $D^0 - \overline{D}^0$ asymmetry as a function of the rapidity in the center-of-mass y^* in pNe collisions at $\sqrt{s_{NN}} = 68.5$ GeV [5]. The error bars represent the quadratic sum of statistical and uncorrelated uncertainties while the grey boxes represent the correlated systematic uncertainties.

where $Y_{corr}(D^0)$ and $Y_{corr}(\overline{D}^0)$ correspond to the efficiency-corrected yields of the $D^0 \to K^-\pi^+$ and $\overline{D}^0 \to K^+\pi^-$ decays respectively. The measured asymmetry is shown in Figure 1 as a function of the center-of-mass rapidity y^*. A negative asymmetry is observed, ranging from $\sim 0\%$ at $y^* = 0$ to $\sim -15\%$ at $y^* \approx -2.5$, although the precision of the measurement is limited by large uncertainties. The experimental results are compared with Pythia 8 [6] predictions which give an asymmetry of about -6%, independent of y^*. An upper limit on the asymmetry is provided by Vogt predictions with (Vogt 1% IC) and without (Vogt no IC) intrinsic charm [7], while the model from Maciula and Szczurek (MS) [4], including 1% of intrinsic charm and 10% of coalescence, reproduces well the trend observed in the data.

4. Results on charmonia production

Charmonium states are produced at the earliest stage of the collision and subsequently probe its entire evolution. They are therefore ideal candidates to study medium effects on hadronization. In heavy-ion collisions, charmonium suppression is commonly associated with the formation of a Quark–Gluon Plasma (QGP). The high density of color charges in the QGP affects the production of $c\bar{c}$ states through color screening, an effect that depends both on the energy density of the collision and on the binding energy of the state. Consequently, the less tightly bound $\psi(2S)$ state is expected to dissociate first, followed by the χ_c, and finally the J/ψ. In addition, a significant fraction of J/ψ originates from the decays of $\psi(2S)$ and χ_c, leading to a multi-step suppression pattern. The measurement of this so-called sequential suppression would provide a key evidence for color screening and the formation of QGP. At very high energies, such as those reached at the LHC, statistical recombination with surrounding $c\overline{c}$ pairs competes with the dissociation mechanism, complicating the interpretation of charmonium suppression. In SMOG collisions, this ambiguity is reduced due

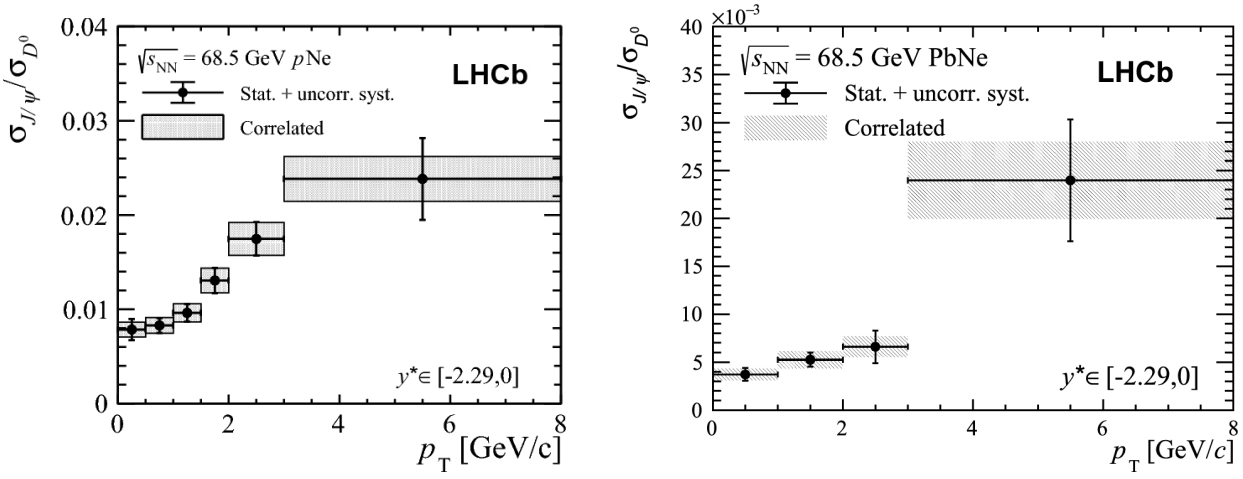

Figure 2: Ratio of J/ψ to D^0 cross-sections as a function of transverse momentum in pNe [8] and PbNe (right) [9] collisions.

to the lower center-of-mass energy, which makes recombination effects negligible. To characterize the suppression observed in fixed-target collisions with a Pb beam, a baseline measurement with a proton beam is required to isolate cold nuclear matter effects. In this context, LHCb has measured the ratio of J/ψ to D^0 cross-sections in pNe [8] and PbNe [9] collisions at $\sqrt{s_{NN}}$ = 68.5 GeV. The results, shown in Figure 2 as a function of transverse momentum, exhibit a strong p_T dependence in both systems, reflecting the differences in the p_T distributions of J/ψ and D^0. In the lowest p_T bins, however, the ratio is smaller in PbNe than in pNe, indicating that J/ψ experiences stronger nuclear effects than D^0 in this system.

The left panel of Figure 3 shows the J/ψ to D^0 cross-section ratio as a function of the product of the beam (A) and target (B) mass numbers. Considering only nuclear effects, the cross-section ratio is expected to follow:

$$\frac{\sigma^{AB}_{J/\psi}}{\sigma^{AB}_{D^0}} = \frac{\sigma^{pp}_{J/\psi}}{\sigma^{pp}_{D^0}} \times (AB)^{\alpha-1} \tag{2}$$

A fit of the data yields $\alpha < 1$, confirming that J/ψ experiences additional nuclear effects compared to D^0.
A similar expression can be derived as a function of the number of binary nucleon-nucleon collisions, N_{coll}, using $N_{coll} = const \times (AB)^{\beta}$. The right panel of Figure 3 shows the cross-section ratio as a function of N_{coll}. Data from PbNe collisions is divided into bins of N_{coll} corresponding to different centrality intervals. A fit to the data yields $\alpha' < 1$, where $\alpha' = (\alpha - 1)/\beta$, indicating again that J/ψ is more affected by nuclear effects than D^0. The trend is consistent across all N_{coll} bins, showing no evidence of J/ψ suppression attributable to QGP formation.

The $\psi(2S)$ has also been measured for the first time in pNe collisions at $\sqrt{s_{NN}}$ = 68.5 GeV [8]. The $\psi(2S)$ / J/ψ integrated ratio is presented in Figure 4 and shows a good agreement with previous measurements for systems with similar mass numbers, despite the limited statistics.

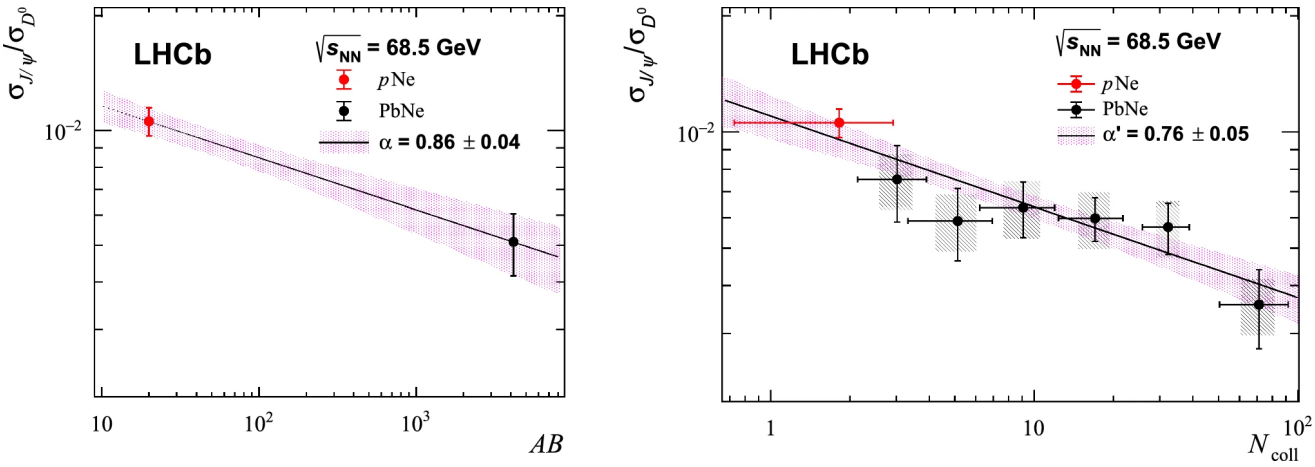

Figure 3: Ratio of J/ψ to D^0 cross-sections in pNe and PbNe collisions, as a function of the product of the beam (A) and target (B) mass numbers (left) and as a function of the number of binary nucleon-nucleon collisions (right) [9].

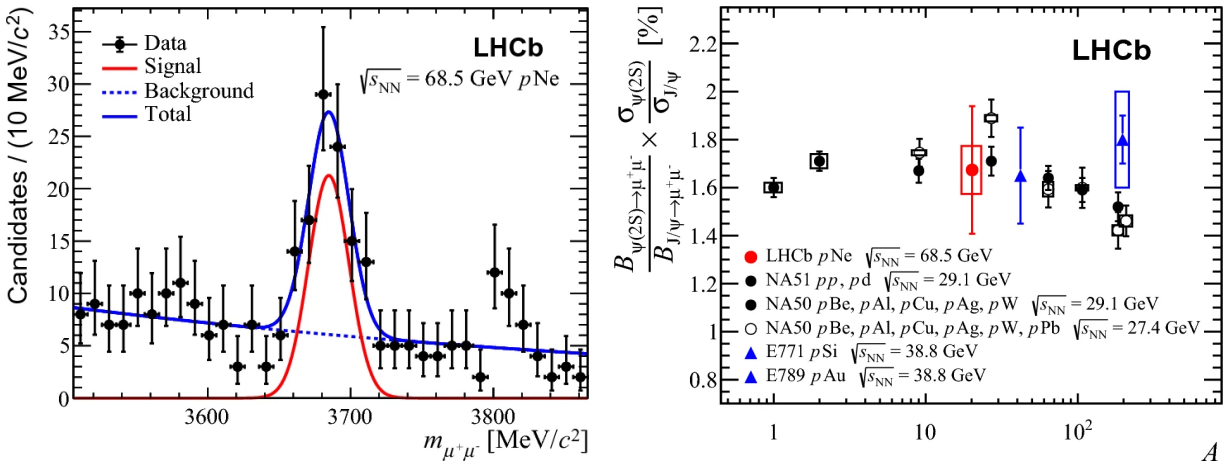

Figure 4: $\psi(2S)$ peak from the dimuon invariant mass spectrum in pNe collisions at $\sqrt{s_{NN}}$ = 68.5 GeV and the corresponding $\psi(2S)$ / J/ψ integrated ratio [8] . The result is compared to other measurements in different systems and center-of-mass energies.

5. The fixed-configuration for Run 3

The fixed-target system of LHCb has been upgraded for Run 3 with the installation of a dedicated gas injection cell called SMOG2 [10]. Its position upstream of the LHCb proton-proton interaction point enables simultaneous data-taking in both collider and fixed-target modes. In addition, the reduced volume of SMOG2 leads to an increased luminosity, improving measurements precision. SMOG2 also offers the possibility to inject non-noble gases, broadening the range of accessible colliding systems.

Since the beginning of the Run 3, LHCb has recorded unprecedented fixed-target samples over a wide range of experimental conditions, including five different gases (H_2, D_2, He, Ar, Ne), four beam types (p, Pb, O, Ne) and two beam energies. The largest fixed-target samples of D^0 and

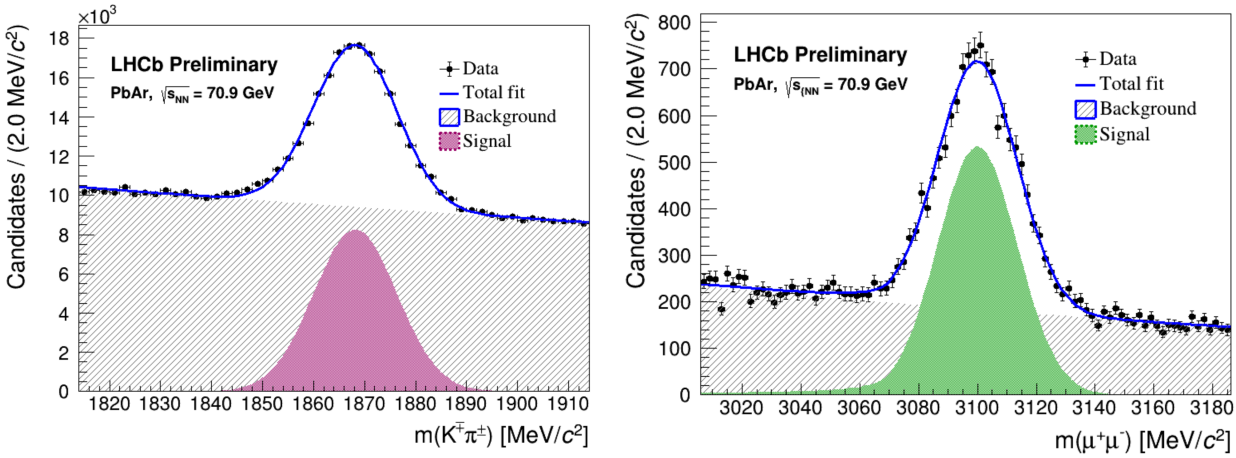

Figure 5: D^0 and J/ψ peaks from PbAr collisions recorded by LHCb at $\sqrt{s_{NN}}$ = 70.9 GeV [11].

J/ψ collected in 2024 in PbAr collisions at $\sqrt{s_{NN}}$ = 70.9 GeV [11] are shown in Figure 5. The enhanced statistics compared to Run 2 will allow more precise measurements of open and hidden charm.

6. Conclusion

The LHCb experiment hosts an innovative fixed-target program at the LHC, providing access to a previously unexplored kinematic region. In particular, it covers the high Bjorken-x region of the target, which offers valuable insight into charm hadronization, while the intermediate center-of-mass energy allows to study charmonia dissociation without significant statistical recombination. These unique physics opportunities were demonstrated with SMOG during the Run 2 of the LHC and will be fully exploited in Run 3, thanks to the upgraded fixed-target setup, SMOG2, delivering larger luminosity over a wide range of collision systems.

References

[1] A. A. Alves et al. (LHCb Collaboration), The LHCb Detector at the LHC. JINST **3**, S08005 (2008). https://doi.org/10.1088/1748-0221/3/08/S08005

[2] R. Aaij et al. (LHCb Collaboration), LHCb Detector Performance. Int. J. Mod. Phys. A **30**, 1530022 (2015). https://doi.org/10.1142/S0217751X15300227

[3] R. Aaij et al. (LHCb Collaboration), Precision luminosity measurements at LHCb. Journal of Instrumentation **9** (2014). https://doi.org/10.1088/1748-0221/9/12/P12005

[4] R. Maciuła, A. Szczurek, Recombination mechanism for D^0-meson production and $D^0 - \overline{D}^0$ production asymmetry in the LHCb p+^{20}Ne fixed-target experiment. Physics Letters B **835** (2022). https://doi.org/10.1016/j.physletb.2022.137530

[5] R. Aaij et al. (LHCb Collaboration), Open charm production and asymmetry in pNe collisions at $\sqrt{s_{NN}}$ = 68.5 GeV. The European Physical Journal C **83**, (2023). http://doi.org/10.1140/epjc/s10052-023-11641-5

[6] T. Sjöstrand et al., A brief introduction to PYTHIA 8.1. Computer Physics Communications **178** (2008). http://dx.doi.org/10.1016/j.cpc.2008.01.036

[7] R. Vogt, Limits on intrinsic charm production from the SeaQuest experiment. Physical Review C **103** (2021). http://doi.org/10.1103/PhysRevC.103.035204

[8] R. Aaij et al. (LHCb Collaboration), Charmonium production in pNe collisions at $\sqrt{s_{NN}}$ = 68.5 GeV. The European Physical Journal C **83** (2023). http://dx.doi.org/10.1140/epjc/s10052-023-11608-6

[9] R. Aaij et al. (LHCb Collaboration), J/ψ and D^0 production in $\sqrt{s_{NN}}$ = 68.5 GeV PbNe collisions. The European Physical Journal C **83** (2023). http://dx.doi.org/10.1140/epjc/s10052-023-11674-w

[10] O. Boente Garcia et al., High-density gas target at the LHCb experiment. Physical Review Accelerators and Beams **27** (2024). http://doi.org/10.1103/PhysRevAccelBeams.27.111001

[11] LHCb Collaboration, J/ψ and D^0 mass peaks in SMOG2 2024 PbAr runs. (2025) https://cds.cern.ch/record/2937139